Journal of Sound and Vibration (2002) **254**(2), 231–244
doi:10.1006/jsvi.2001.3938, available online at http://www.idealibrary.com on IDEAL®

SOLUTION OF COUPLED ACOUSTIC PROBLEMS: A PARTIALLY OPENED CAVITY COUPLED WITH A MEMBRANE AND A SEMI-INFINITE EXTERIOR FIELD

Y.-H. KIM AND S.-M. KIM

Center for Noise and Vibration Control (*NOVIC*), *Department of Mechanical Engineering*, *Korea Advanced Institute of Science and Technology* (*KAIST*), 373-1 *Science Town*, *Taejon* 305-701, *Korea. E-mail*: *yhkim@sorak.kaist.ac.kr*

(*Received* 7 *April* 2000, *and in final form* 3 *April* 2001)

There have been many attempts to understand the coupling phenomena between a solid structure and the surrounding fluid. However, the studies were restricted to interaction only between a structure and a finite cavity or a structure and acoustic field of infinite size. The system that we have studied has a structure that faces both a cavity of finite size and an external field of semi-infinite size. We also allow a hole, which can directly interact with the cavity as well as the external field. This configuration, therefore, provides two different interactions, or communication means. One is the finite structure and the other is the hole of finite size. This paper studies as to how these two components interact with the other two systems: the finite cavity covered by the structure and the hole, and the semi-infinite fluid. For simplicity, a two-dimensional and partially opened cavity coupled with a membrane and an exterior field was selected. The solution has to be found by solving a boundary value problem, but this case has to do with the boundaries that have two different conditions: one is the membrane and the other is the hole. The solution has been found in terms of the modal functions that satisfy the boundary conditions of finite cavity, membrane and hole. Non-dimensional coupling coefficients are obtained from the solution. The results exhibit that the coupling effect gives additional peaks and troughs in the averaged pressure of the cavity. These peaks and troughs are symmetrically arranged with respect to Helmholtz frequency of the cavity. The strong coupling occurs at the trough frequencies where the membrane interacts actively with the cavity and the exterior field.

1. INTRODUCTION

The sound pressure field in a cavity is affected not only by acoustic sources in the cavity but also by the acoustic characteristics of the cavity walls. One of the simplest examples of these systems is the cavity whose cross-sectional area is rectangular or circular and whose walls are acoustically rigid. This configuration makes it possible to analyze the system by using well-known functions such as harmonic functions (for example, see reference [1]). When absorbent material is attached to part or all of the wall surface, we can analyze the system mathematically by assuming the wall as locally reacting and having a small absorption coefficient [1]. However, if the walls include a flexible structure, we must consider them as having extensively reacting boundary conditions. This structural–acoustic coupling makes it difficult for us to obtain the solutions because their corresponding governing equations have to be solved simultaneously.

Studies on structural–acoustic coupling have been done very extensively. For example, Dowell and Voss [2] tried to analyze a cavity-backed plate and Lyon [3] studied the effect

0022-460X/02/$35.00

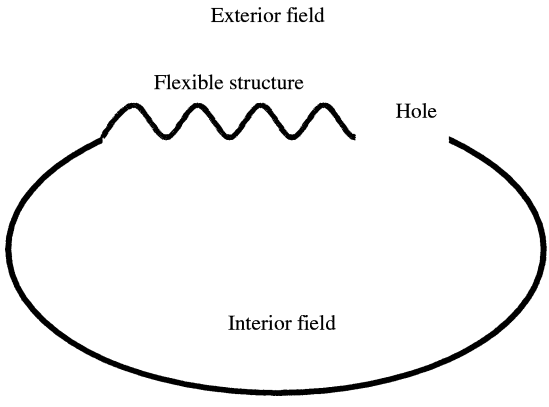

Figure 1. The coupling system that has four subsystems (an interior, an exterior, hole and a flexible structure). The hole allows direct interaction between the interior and the exterior.

of a flexible wall on a cavity. Pretlove [4, 5] derived an expression for the cavity-backed plate vibration using *in-vacuo* modes. De Rosa *et al.* [6] reviewed the basic methodologies for the study of the vibroacoustic problem of enclosed cavities. The cavity has one elastic wall in the low modal density frequency region. The acoustic coupling between finite cavity and exterior field has also been studied extensively in musical acoustics. For example, a guitar and violin have been studied [7–11]. All these studies considered the interaction between a structure and a cavity of finite size and neglected and effect of external fields of infinite size. Seybert *et al.* [12] attempted to obtain the solution of coupled interior/exterior acoustic problems. They used the boundary element method that can handle continuity conditions at the interface surface between two domains. However, it is not able to consider a structural vibration at the interface. Guy [13] investigated acoustic energy from an external field to a cavity through a panel. However, neglected the mutual interaction between the cavity and the external field. Morse [14] studied the interaction between a membrane and external fields. The important point of his study is that it considered incident and transmitted waves propagating in the infinite field. These studies certainly provided many useful results so that we can understand the coupled acoustic problem. However, those are very limited, therefore cannot cope with general coupled acoustic problem, which can be illustrated as in Figure 1.

In this paper, we attempt to study the coupling system that has a cavity which is covered by a hole and a flexible structure. The difficulty in the analysis arises not only because there is a structural–acoustic coupling but also because there is an interaction between the cavity and the exterior. Although there has been an experimental approach using the acoustic holographic method [15], no study has been done theoretically, except the ones with simplified models [16, 17]. For this reason, we have studied a simple coupling system as shown in Figure 2. For simplicity, a membrane was chosen as a structure. When a plate is used instead of the membrane, the second order governing equation in replaced with the fourth order one. This would lead us to have different modal functions, which include exponential expression additionally. Because their values are decaying as the calculation points go far from the boundaries, we can say that the difference occurs only around the boundaries, compared with the mode shapes for a membrane. This paper has attempted to investigate the structural–acoustic coupling mechanism by using as simple a case as possible, so that we can highlight our study on the coupling. The next study will have to do with the structure that has more complicated mode shapes. However, it is noteworthy that the basic formulation and solution method will be the same if we try to express the

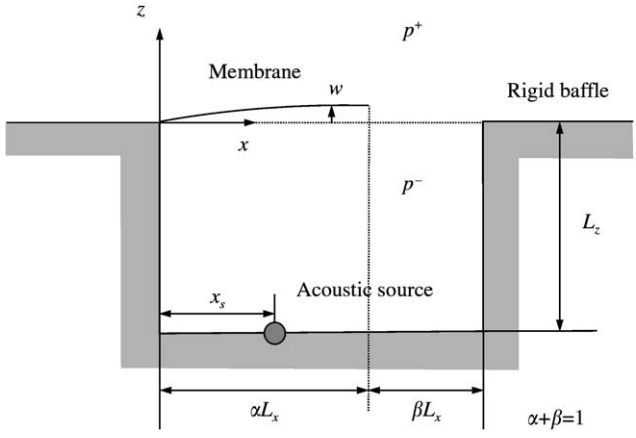

Figure 2. The two-dimensional coupling system used in the study: a partially opened cavity coupled with a membrane and a semi-infinite exterior field.

structural vibration and acoustic pressure field by using orthonormal functions, or mode shapes. One boundary condition of the membrane is free, so that we can have a hole, starting from the end of the membrane to the wall of the cavity (Figure 2). The free boundary condition may be envisaged by connecting the membrane at the free end to the other side of the hole by using massless strings.

The objective of our study is to understand the coupling effect in a general structural–acoustic coupling system. To meet this objective, we derived the governing equations that can express the structure, hole, cavity and exterior field. The difficult part in the analysis is that we have to handle two different boundary conditions at the interface (Figure 2). This mathematically means that we have more equations than unknowns. This rather challenging problem has been solved by utilizing the modal functions of the membrane, hole, and the cavity so that the number of equations and number of unknowns in the modal domain are the same. The details are given in section 3.

The contribution and highlight of this paper are that it provides the coupling measures. They show as to how the finite cavity communicates with the exterior field through the vibrating structure and the hole. These communications depend on frequency, therefore wavenumber and wavelength.

2. GOVERNING EQUATIONS FOR THE COUPLING SYSTEM UNDER STUDY

2.1. DESCRIPTIONS OF THE COUPLING SYSTEM

The coupling system used in this study is composed of four parts: a cavity, a membrane, a hole, and a semi-infinite space (Figure 2). We assume that the system does not depend on y direction. In other words, the analysis is restricted to a two-dimensional case for its simplicity. The cavity is rectangular and its size is L_x by L_z. Its walls are assumed to be acoustically rigid except the top wall ($z = 0, 0 < x < L_x$). The top of the cavity is partially covered by a membrane ($z = 0, 0 < x < \alpha L_x, 0 < \alpha < 1$) and the other part ($z = 0, \alpha L_x < x < L_x$) remains open so that direct interaction occurs between the cavity and the outer semi-infinite acoustic field ($z > 0$). One end ($x = 0$) of the membrane is fixed to the cavity and the other end ($x = \alpha L_x$) is free. The thickness of the membrane is regarded as negligible compared with the shortest wavelength of interest. The outer field is semi-infinite

and its lower boundary ($z = 0$, $x < 0$ and $x > L_x$) is assumed to be a rigid baffle. The system is excited by a monopole source which is located at the bottom of the cavity ($z = -L_z$, $x = x_s$). The monopole strength (volume velocity of the source) is Q.

2.2. GOVERNING EQUATIONS AND BOUNDARY CONDITIONS

Assuming harmonic time dependence $e^{j\omega t}$, we can obtain the governing equations for the acoustic fields and the membrane as

$$\left(\frac{\partial^2}{\partial x^2} + \frac{\partial^2}{\partial z^2} + k^2\right) p^-(x, z) = 0 \quad \text{(inside the cavity)}, \tag{1}$$

$$\left(\frac{\partial^2}{\partial x^2} + \frac{\partial^2}{\partial z^2} + k^2\right) p^+(x, z) = 0 \quad \text{(outside the cavity)}, \tag{2}$$

$$\left(\frac{\mathrm{d}^2}{\mathrm{d}x^2} + \kappa^2\right) w(x) = -\frac{1}{T}\{p^-(x, 0) - p^+(x, 0)\} \quad \text{(on the membrane, } 0 < x < \alpha L_x), \tag{3}$$

where p^-, p^+, and w represent pressure inside and outside the cavity and membrane displacement, k and κ represent the wavenumber in the acoustic fields and the membrane, and T denotes the tension acting in the membrane. The equations for the boundary conditions at the left, right and bottom walls of the cavity are

$$\left.\frac{\partial p^-}{\partial x}\right|_{x=0} = \left.\frac{\partial p^-}{\partial x}\right|_{x=L_x} = 0. \tag{4a, b}$$

$$\left.\frac{\partial p^-}{\partial z}\right|_{z=-L_z} = -\mathrm{j}k\rho c Q\delta(x - x_s). \tag{5}$$

Since the rigid baffle is located at $z = 0$, the following boundary condition must be satisfied:

$$\left.\frac{\partial p^+}{\partial z}\right|_{z=0} = 0 \quad (x < 0, x > L_x). \tag{6}$$

The boundary conditions for the membrane are

$$w|_{x=0} = 0, \quad \left.\frac{\mathrm{d}w}{\mathrm{d}x}\right|_{x=\alpha L_x} = 0. \tag{7a, b}$$

On the membrane surface ($0 < x < \alpha L_x$) the velocity continuity must be satisfied. At the hole ($\alpha L_x < x < L_x$), pressure and particle velocities must be continuous. These lead to the following equations:

$$\left.\frac{\partial p^-}{\partial z}\right|_{z=0} = \rho\omega^2 w, \quad \left.\frac{\partial p^+}{\partial z}\right|_{z=0} = \rho\omega^2 w \quad (0 < x < \alpha L_x), \tag{8a, b}$$

$$p^-|_{z=0} = p^+|_{z=0}, \quad \left.\frac{\partial p^-}{\partial z}\right|_{z=0} = \left.\frac{\partial p^+}{\partial z}\right|_{z=0} \quad (\alpha L_x < x < L_x). \tag{9a, b}$$

We now have three governing equations (equations (1–3)), and rather complicated boundary conditions (equations (4–9)). The next section attempts to solve this boundary value problem.

3. MATRIX EQUATION FOR MODEL COEFFICIENTS

The cavity pressure can be expressed by the superposition of $e^{-jk_x x}e^{-jk_z z}$, $e^{-jk_x x}e^{+jk_z z}$, $e^{+jk_x x}e^{-jk_z z}$, and $e^{-jk_x x}e^{-jk_z z}$, where $k_x^2 + k_z^2 = k^2$. These represent positive- and negative-going parts of x and z directional waves. By applying the left and right boundary conditions of the cavity (equations (4a) and (4b)), the pressure inside the cavity can be written as

$$p^-(x, z) = \sum_{n=0}^{\infty} \cos k_{xn} x (P_n^+ e^{-jk_{zn} z} + P_n^- e^{jk_{zn} z}), \tag{10}$$

$$k_{xn}^2 + k_{zn}^2 = k^2, \quad k_{xn} = \frac{n\pi}{L_x}, \tag{11a, b}$$

$$k_{zn} = \begin{cases} \sqrt{k^2 - k_{xn}^2}, & k^2 > k_{xn}^2, \\ -j\sqrt{k_{xn}^2 - k^2}, & k^2 < k_{xn}^2, \end{cases} \tag{11c}$$

where k_{xn} and k_{zn} are x and z directional wavenumbers of the nth mode respectively. P_n^+ and P_n^- represent positive- and negative-going modal coefficients of the nth mode.

Pressure outside the cavity can be derived from the Kirchhoff–Helmholtz integral equation (for example, see reference [18]), i.e.,

$$p^+(x, z) = -\int_{-\infty}^{\infty} \left\{ G(x, z|\xi, 0) \frac{\partial p^+(\xi, 0)}{\partial \zeta} - p^+(\xi, 0) \frac{\partial G(x, z|\xi, 0)}{\partial \zeta} \right\} d\xi, \tag{12}$$

where $G(x, z|\xi, \zeta)$ is any Green's function which satisfies

$$\left(\frac{\partial^2}{\partial x^2} + \frac{\partial^2}{\partial z^2} + k^2 \right) G(x, z|\xi, \zeta) = -\delta(x - \xi)\delta(z - \zeta). \tag{13}$$

We may choose Green's function that satisfies the Neumann boundary condition at $z = 0$ (equation (6)). Then the second term of equation (12) vanishes. Therefore, equation (12) can rewritten as

$$p^+(x, z) = -\int_0^{L_x} G(x, z|\xi, 0) \frac{\partial p^+(\xi, 0)}{\partial \zeta} d\xi, \tag{14}$$

$$G(x, z|\xi, 0) = -\frac{j}{2} H_0^{(2)}(kr), \quad r = \sqrt{(x - \xi)^2 + z^2}. \tag{15a, b}$$

The integration region has to be $0 < x < L_x$ in equation (14). This is simple because the z directional derivatives of pressure is zero in the region $x < 0$ and $x > L_x$. Here, $H_0^{(2)}(\cdot)$ is the second kind Hankel function of order zero that obviously satisfies the Neumann boundary condition at $z = 0$.

On the other hand, the membrane displacement can be tried to be expressed as

$$w(x) = \sum_{m=0}^{\infty} W_m \sin \kappa_m x, \qquad \kappa_m = \frac{(2m + 1)\pi}{2\alpha L_x}. \tag{16, 17}$$

This satisfies the corresponding boundary conditions (equations 7(a) and 7(b)). We now have expressions for the pressure, inside of the cavity (p^-, equation (10)), outside of the cavity (p^+, equation (14)), and for the membrane displacement (w, equation (16)). All unknowns of these expressions have to be determined according to the corresponding boundary conditions. Next, detailed procedures are described.

On inserting equation (10) into equation (5) we obtain

$$\mathrm{j}\sum_{n=0}^{\infty} k_{zn}\cos k_{xn}x(-P_n^+\mathrm{e}^{\mathrm{j}k_{zn}L_z}+P_n^-\mathrm{e}^{-\mathrm{j}k_{zn}L_z}) = -\mathrm{j}k\rho cQ\delta(x-x_s) \quad (0<x<L_x) \tag{18}$$

and substituting equation (10) into equation (3) and by using equations (14), (16), (8) and (9) we have

$$T\sum_{m=0}^{\infty} W_m(\kappa_m^2-\kappa^2)\sin\kappa_m x = \sum_{n=0}^{\infty}\cos k_{xn}x(P_n^+ + P_n^-) + \sum_{n=0}^{\infty}\int_0^{L_x}\frac{\mathrm{j}}{2}H_0^{(2)}(k|x-\xi|)\mathrm{j}k_{zn}\cos k_{xn}\xi(-P_n^+ + P_n^-)\,\mathrm{d}\xi \quad (0<x<\alpha L_x). \tag{19}$$

Again substituting equation (10) into equation (8a) and by using equation (9b) we have

$$\mathrm{j}\sum_{n=0}^{\infty} k_{zn}\cos k_{xn}x(-P_n^+ + P_n^-) = \rho\omega^2\sum_{m=0}^{\infty} W_m\sin\kappa_m x \quad (0<x<\alpha L_x). \tag{20}$$

By substituting equation (10) into equation (9a) and by using equation (9b) we have

$$\sum_{n=0}^{\infty}\cos k_{xn}x(P_n^+ + P_n^-) = -\sum_{n=0}^{\infty}\int_0^{L_x}\frac{\mathrm{j}}{2}H_0^{(2)}(k|x-\xi|)\mathrm{j}k_{zn}\cos k_{xn}\xi(-P_n^+ + P_n^-)\,\mathrm{d}\xi$$

$$(\alpha L_x < x < L_x). \tag{21}$$

Now, we have four equations (equations (18–21)), while having three unknown coefficients, P_n^+, P_n^-, and W_m. This rather difficult problem is due to the dual boundary condition on the surface $z=0$. That is, one is the membrane and the other is the hole. It is noteworthy that the number of unknowns has also to do with the indexes n and m. This is essentially related to the way in which the acoustic cavity interacts with the membrane. The solutions, in other words, determining the three groups of unknown coefficients, have to be found by utilizing the orthogonal functions that are used in equations (18)–(21). Next, the details of the method which we pursue to obtain the solution are given.

Firstly, we multiply equation (18) by $\cos(k_{xn'}x)$ and then integrate it from 0 to L_x. This leads to

$$\mathrm{j}k_{zn}\frac{L_x}{\varepsilon_n}(-P_n^+\mathrm{e}^{\mathrm{j}k_{zn}L_z}+P_n^-\mathrm{e}^{-\mathrm{j}k_{zn}L_z}) = -\mathrm{j}k\rho cQ\cos k_{xn}x_s, \tag{22}$$

$$P_n^+ = P_n^-\mathrm{e}^{-2\mathrm{j}k_{zn}L_z} + \frac{\mathrm{j}k\rho cQ\varepsilon_n}{\mathrm{j}k_{zn}L_x}\cos k_{xn}x_s\mathrm{e}^{-\mathrm{j}k_{zn}L_z}, \tag{23}$$

$$\varepsilon_n = \begin{cases} 1 & n=0, \\ 2 & n=1,2,3,\ldots. \end{cases} \tag{24}$$

Similarly, multiplying equation (19) by $\sin(\kappa_{m'}x)$ and integrating it from 0 to αL_x, readily gives us

$$\frac{\alpha T W_m}{2}(\kappa_m^2 - \kappa^2) = \sum_{n=0}^{\infty}(P_n^+ + P_n^-)\bar{\mu}_{mn} + \sum_{n=0}^{\infty} k_{zn}L_x(-P_n^+ + P_n^-)\bar{a}_{mn}, \tag{25}$$

$$\bar{\mu}_{mn} = \int_0^{\alpha} \sin\frac{(2m+1)\pi x}{2\alpha}\cos n\pi x\,\mathrm{d}x$$

$$= \begin{cases} \dfrac{\alpha}{(2m+1)\pi}, & 2m+1 = 2\alpha n, \\ \dfrac{\alpha\{1-(-1)^m\sin\alpha n\pi\}}{(2m+1-2\alpha n)\pi} + \dfrac{\alpha\{1+(-1)^m\sin\alpha n\pi\}}{(2m+1+2\alpha n)\pi}, & 2m+1 \neq 2\alpha n, \end{cases} \tag{26}$$

$$\bar{a}_{mn} = -\int_0^1 \mathrm{d}\xi \int_0^{\alpha} \mathrm{d}x \left\{\sin\frac{(2m+1)\pi x}{2\alpha}\cos n\pi\xi \times \frac{1}{2}H_0^{(2)}(kL_x|x-\xi|)\right\}. \tag{27}$$

Equation (25) contains two non-dimensional coupling coefficients, $\bar{\mu}_{mn}$ and $\bar{a}_{mn}$. The first coefficient $\bar{\mu}_{mn}$ represents the component of the mth membrane mode for the nth cavity mode or *vice versa*. The second coefficient $\bar{a}_{mn}$ expresses the modal contributions, membrane and cavity mode, of the Green function (equation (15)). We could also say that, $\bar{a}_{mn}$ represents the degree of participation of mth modal component to nth cavity mode when it propagates.

As we have done before, multiplying equation (20) by $\sin(\kappa_{m'}x)$ and integrating it from 0 at αL_x we obtain

$$\mathrm{j}\sum_{n=0}^{\infty} k_{zn}(-P_n^+ + P_n^-)\bar{\mu}_{mn} = \rho\omega^2 W_m \frac{\alpha}{2}. \tag{28}$$

Finally, multiplying equation (21) by $\sin\kappa'_m(L_x - x)$ and integrating if from αL_x to L_x, where we have the hole, we obtain

$$\sum_{n=0}^{\infty}(P_n^+ + P_n^-)\bar{v}_{nm} = -\sum_{n=0}^{\infty} k_{zn}L_x(-P_n^+ + P_n^-)\bar{b}_{mn}, \tag{29}$$

$$\bar{v}_{mn} = \int_{\alpha}^1 \sin\frac{(2m+1)\pi(1-x)}{2\beta}\cos n\pi x\,\mathrm{d}x$$

$$= \begin{cases} (-1)^n\dfrac{\beta}{(2m+1)\pi} & 2m+1 = 2\beta n, \\ (-1)^n\left[\dfrac{\beta\{1-(-1)^m\sin\beta n\pi\}}{(2m+1-2\beta n)\pi} + \dfrac{\beta\{1+(-1)^m\sin\beta n\pi\}}{(2m+1+2\beta n)\pi}\right], & 2m+1 \neq 2\beta n, \end{cases} \tag{30}$$

$$\bar{b}_{mn} = -\int_0^1 \mathrm{d}\xi \int_{\alpha}^1 \mathrm{d}x \left\{\sin\frac{(2m+1)\pi(1-x)}{2\beta}\cos n\pi\xi \times \frac{1}{2}H_0^{(2)}(kL_x|x-\xi|)\right\}. \tag{31}$$

Equation (29) has two non-dimensional coupling coefficients, $\bar{v}_{mn}$ and $\bar{b}_{mn}$. The first coefficient $\bar{v}_{mn}$ represents the mth modal component ($\sin(\kappa_m x)$) of the nth cavity mode. Compared to $\bar{\mu}_{mn}$, this expresses the modal contribution of the hole and the cavity. These

two coefficients $\bar{v}_{mn}$ and $\bar{\mu}_{mn}$ are real and functions of only m, n and α. The second coefficient $\bar{b}_{mn}$ has characteristics similar to $\bar{a}_{mn}$, but expresses the role of the hole and the cavity. It is noteworthy that the integral regions are different (equations (26), (27), (30) and (31)).

If we eliminate P_n^+ and W_m in equations (22), (25), (28) and (29), then we have equations only in terms of P_n^-, i.e.,

$$\sum_{n=0}^{\infty} \mathrm{j}k_{zn} s_m \left(-P_n^- + P_n^- \mathrm{e}^{-2\mathrm{j}k_{zn}L_z} + \frac{\mathrm{j}k\rho cQ\varepsilon_n}{\mathrm{j}k_{zn}L_x} \cos k_{xn}x_s \mathrm{e}^{-\mathrm{j}k_{zn}L_z} \right) \bar{\mu}_{mn}$$

$$= \sum_{n=0}^{\infty} \left[P_n^- \{ \bar{\mu}_{mn} + k_{zn}L_x \bar{a}_{mn} \} + \left(P_n^- \mathrm{e}^{-2\mathrm{j}k_{zn}L_z} + \frac{\mathrm{j}k\rho cQ\varepsilon_n}{\mathrm{j}k_{zn}L_x} \cos k_{xn}x_s \mathrm{e}^{-\mathrm{j}k_{zn}L_z} \right) \{ \bar{\mu}_{mn} - k_{zn}L_x \bar{a}_{mn} \} \right], \tag{32}$$

$$\sum_{n=0}^{\infty} \left(P_n^- + P_n^- \mathrm{e}^{-2\mathrm{j}k_{zn}L_z} + \frac{\mathrm{j}k\rho cQ\varepsilon_n}{\mathrm{j}k_{zn}L_x} \cos k_{xn}x_s \mathrm{e}^{-\mathrm{j}k_{zn}L_z} \right) \bar{v}_{mn}$$

$$= -\sum_{n=0}^{\infty} \left[\left(P_n^- - P_n^- \mathrm{e}^{-2\mathrm{j}k_{zn}L_z} - \frac{\mathrm{j}k\rho cQ\varepsilon_n}{\mathrm{j}k_{zn}L_x} \cos k_{xn}x_s \mathrm{e}^{-\mathrm{j}k_{zn}L_z} \right) k_{zn}L_x \bar{b}_{mn} \right]. \tag{33}$$

Here, the variable s_m is

$$s_m = \frac{T\left(\kappa_m^2 - \kappa^2\right)}{\rho\omega^2} = \frac{\rho_m}{\rho} \left\{ \left(\frac{\kappa_m}{\kappa} \right)^2 - 1 \right\} \tag{34}$$

and it has the dimension of length.

We can rewritten equations (32) and (33) in a more compact form. This has to do with a matrix form for the coefficient P_n^-. This can be readily obtained as

$$[A_{mn}^I]\{P_n^-\} = \{Q_m^{I\alpha}\}, \qquad [B_{mn}^I]\{P_n^-\} = \{Q_m^{I\beta}\}, \tag{35a, b}$$

where the elements of each matrix are

$$A_{mn}^I = \mathrm{j}k_{zn}s_m(1 - \mathrm{e}^{-2\mathrm{j}k_{zn}L_z})\bar{\mu}_{mn} + (1 + \mathrm{e}^{-2\mathrm{j}k_{zn}L_z})\bar{\mu}_{mn} + (1 - \mathrm{e}^{-2\mathrm{j}k_{zn}L_z})k_{zn}L_x\bar{a}_{mn}, \tag{36a}$$

$$B_{mn}^I = (1 + \mathrm{e}^{-2\mathrm{j}k_{zn}L_z})\bar{v}_{mn} + (1 - \mathrm{e}^{-2\mathrm{j}k_{zn}L_z})k_{zn}L_x\bar{b}_{mn}, \tag{36b}$$

$$Q_m^{I\alpha} = \mathrm{j}k\rho cQ \sum_{n=0}^{\infty} \{ \mathrm{j}k_{zn}s_m\bar{\mu}_{mn} - (\bar{\mu}_{mn} - k_{zn}L_x\bar{a}_{mn}) \} \frac{\varepsilon_n}{\mathrm{j}k_{zn}L_x} \cos k_{xn}x_s \mathrm{e}^{-\mathrm{j}k_{zn}L_z}, \tag{36c}$$

$$Q_m^{I\beta} = -\mathrm{j}k\rho cQ \sum_{n=0}^{\infty} (\bar{v}_{mn} - k_{zn}L_x\bar{b}_{mn}) \frac{\varepsilon_n}{\mathrm{j}k_{zn}L_x} \cos k_{xn}x_s \mathrm{e}^{-\mathrm{j}k_{zn}L_z}. \tag{36d}$$

The characteristics of the coupling system can be readily understood by using the solutions of equations (35a, b). As we mentioned before, the number of equations (equations (35a, b)) is larger than the number of unknowns (P_n^-). In other words, P_n^- has to satisfy two equations. It is noteworthy, however, that equations (35a, b) are in fact in matrix form. Therefore, the actual number of unknowns has to be determined by how many P_n^- terms we want to obtain. The number of P_n^- terms has to do with the modal density for a selected excitation frequency: the frequency of the acoustic source. In practice, we may, however, attempt to start with an arbitrary number, then increase the number until we have the result

that is not sensitive to the increase. We can solve this problem by using the same number of modes and equations. If we want to obtain $N+1$ coefficients P_n^- $(n=0,\ldots,N)$, then we may use M equations (35a) and $N+1-M$ equations (35b). The number M and $N+1-M$ are the ones which makes all three modal functions (cavity, membrane, and hole) have nearly same wavenumbers. The simulations performed in section 5 were obtained by this method.

4. PROPERTIES OF PARAMETERS AND LIMIT CHECKS

4.1. COUPLING COEFFICIENTS

There are four coupling coefficients: $\bar{\mu}_{mn}$, $\bar{\nu}_{mn}$, $\bar{a}_{mn}$, and $\bar{b}_{mn}$. The coefficient $\bar{\mu}_{mn}$ is a non-dimensional real-valued function of m, n, and α. It represents the mth modal component of $\phi_m(x)=(2m+1)\pi x/2\alpha$ (modal function of the membrane) with regard to nth mode, $\psi_n(x)=\cos n\pi x$ (modal function for the cavity), or *vice versa*. Whether or not it satisfies the relation $2m+1=2\alpha n$, it has a different expression (see equation (26)). As $2m+1$ goes to $2\alpha n$, the expression for $2m+1\neq 2\alpha n$ converges to the expression for $2m+1=2\alpha n$. Thus, $\bar{\mu}_{mn}$ is a continuous function if m and n are real independent variables. By comparing the first expression with the second one, we can learn that the first one tends to have a maximum value when $2m+1=2\alpha n$. This means that $\bar{\mu}_{mn}$ has the maximum value when $n=(2m+1)/2\alpha$. In other words, the coupling between $\phi_m(x)$ and $\psi_n(x)$ will be strong when the wavenumbers are the same. As m or n goes to infinity, $\bar{\mu}_{mn}$ goes to 0 with the speed of $1/m$ or $1/n$. This means that a higher mode makes the coupling effect between a membrane and cavity smaller. When $\alpha=0$, so is $\bar{\mu}_{mn}$. This is a very straightforward result. It simply means that if there is no membrane, then there is no chance for a cavity to interact with a membrane. A similar behavior can be observed for the coefficient $\bar{\nu}_{mn}$. It is a non-dimensional real-valued function of m, n, and α (or β). It has the maximum value when $n=(2m+1)/2\beta$ and it goes to zero as m and n becomes smaller. If $\beta=0$ (or $\alpha=1$), then $\bar{\nu}_{mn}$ is zero. This means that the interaction between the cavity and hole (or outer domain) is not possible.

$\bar{a}_{mn}$ is a function of m, n, α and kL_x. It is noteworthy that $\bar{a}_{mn}$ is a complex value and dependent on the cavity length divided by the wavelength. This is because $\bar{a}_{mn}$ includes a function $H_0^{(2)}(kL_x|x-\xi|)$. We can obtain the distribution of sound pressure along the x-axis from 0 to 1 when monopole sources are distributed along the x-axis from 0 to α and their strength is equal to $\phi_m(x)$. $\bar{a}_{mn}$ is the nth modal component $(\psi_n(x))$ of the pressure distribution. It also represents the coupling between the membrane and cavity modes such as $\bar{\mu}_{mn}$ does. However, it represents the effect of propagation. Therefore, when $\alpha=0$, so is $\bar{a}_{mn}$. This means that there is no interaction between a membrane and a cavity.

The last coefficient $\bar{b}_{mn}$ has properties similar to $\bar{a}_{nm}$. It is a non-dimensional complex-valued function of m, n, α and kL_x. It is the nth modal component $(\psi_n(x))$ of the pressure field along the x-axis $(0<x<1)$ that is made by the monopole of strength $\phi_m(x)$, which is distributed along the x-axis $(\alpha<x<1)$. It goes to zero as β is taken as 0^+ (or α as 1^-). This means that there is no interaction between a cavity and the field outside the cavity.

4.2. LENGTH PARAMETER s_m

The parameter s_m (equation (34)) has a length dimension and interesting limit values. As κ goes to infinity or a frequency increases, s_m approaches $-\rho_m/\rho$. This indicates that

TABLE 1

Limiting values of s_m for several cases

Limiting cases	Limiting values of s_m
$\kappa = \dfrac{\omega}{c_m} = \dfrac{\omega\sqrt{\rho_m}}{\sqrt{T}} \to \infty$	$s_m \to -\dfrac{\rho_m}{\rho}$
$\kappa = \dfrac{\omega}{c_m} = \dfrac{\omega\sqrt{\rho_m}}{\sqrt{T}} \to 0$	$s_m \to \dfrac{\rho_m}{\rho}\left(\dfrac{\kappa_m}{\kappa}\right)^2 = \dfrac{T\kappa_m^2}{\rho\omega^2}$
$\kappa_m = \dfrac{(2m+1)\pi}{2\alpha L_x} \to \infty$	$s_m \to \dfrac{\rho_m}{\rho}\left(\dfrac{\kappa_m}{\kappa}\right)^2 = \dfrac{T\kappa_m^2}{\rho\omega^2}$
$\kappa_m = \kappa$	$s_m = 0$
$\rho \to \infty$	$s_m \to 0$
$\alpha, \rho, \omega \to 0, m, \rho_m, T \to \infty$	$s_m \to \infty$

TABLE 2

Limiting values of A_{mn} and B_{mn} for several cases

Limiting cases	Limiting values of A_{mn} and B_{mn}
$k_{zn}L_z \to 0$	$A_{mn} \to -2\bar{\mu}_{mn}$
	$B_{mn} \to -2\bar{\nu}_{mn}$
$k_{zn}L_z \to \infty$	$A_{mn} \to (\mathrm{j}k_{zn}s_m + 1)\bar{\mu}_{mn} - k_{zn}L_x\bar{a}_{mn}$
	$B_{mn} = \bar{\nu}_{nm} - k_{zn}L_x\bar{b}_m$
$k_{zn}L_x \to 0$	$A_{mn} \to \{-\mathrm{j}k_{zn}s_m(1 - \mathrm{e}^{-2\mathrm{j}k_{zn}L_z}) - (1 + \mathrm{e}^{-2\mathrm{j}k_{zn}L_z})\}\bar{\mu}_{mn}$
	$B_{mn} \to (1 + \mathrm{e}^{-2\mathrm{j}k_{zn}L_z})\bar{\nu}_{mn}$
$k_{zn}L_x \to \infty$	$A_{mn} \to -(1 - \mathrm{e}^{-2\mathrm{j}k_{zn}L_z})k_{zn}L_x\bar{a}_{mn}$
	$B_{mn} \to -(1 - \mathrm{e}^{-2\mathrm{j}k_{zn}L_z})k_{zn}L_x\bar{b}_m$
$k_{zn}s_m \to 0$	$A_{mn} \to -(1 + \mathrm{e}^{-2\mathrm{j}k_{zn}L_z})\bar{\mu}_{mn} - (1 - \mathrm{e}^{-2\mathrm{j}k_{zn}L_z})k_{zn}L_x\bar{a}_{mn}$
	$B_{mn} = (1 + \mathrm{e}^{-2\mathrm{j}k_{zn}L_z})\bar{\nu}_{mn} - (1 - \mathrm{e}^{-2\mathrm{j}k_{zn}L_z})k_{zn}L_x\bar{b}_{mn}$
$k_{zn}s_m \to \infty$	$A_{mn} \to -\mathrm{j}k_{zn}s_m(1 - \mathrm{e}^{-2\mathrm{j}k_{zn}L_z})\bar{\mu}_{mn}$
	$B_{mn} = (1 + \mathrm{e}^{-2\mathrm{j}k_{zn}L_z})\bar{\nu}_{mn} - (1 - \mathrm{e}^{-2\mathrm{j}k_{zn}L_z})k_{zn}L_x\bar{b}_{mn}$

s_m depends only on the ratio of the density of the membrane to the density of the acoustic media in the cavity, for example, air. This means that the mass effect becomes dominant at a high frequency. On the other hand, as κ goes to zero, s_m approaches $T\kappa_m^2/\rho\omega^2$. This depends on the ratio of membrane tension to the acceleration force subjected to the air. The other interesting results are summarized in Table 1.

4.3. LIMITING VALUES OF A_{mn} AND B_{mn} FOR VARIOUS CASES RELATED TO THE VARIABLE k_{zn}

As $k_{zn}L_z$ goes to zero, A_{mn} and B_{mn} have a tendency to depend only on $\bar{\mu}_{mn}$ and $\bar{\nu}_{mn}$. The disappearance of $\bar{a}_{mn}$ and $\bar{b}_{mn}$ means that the vibration of the membrane is no longer

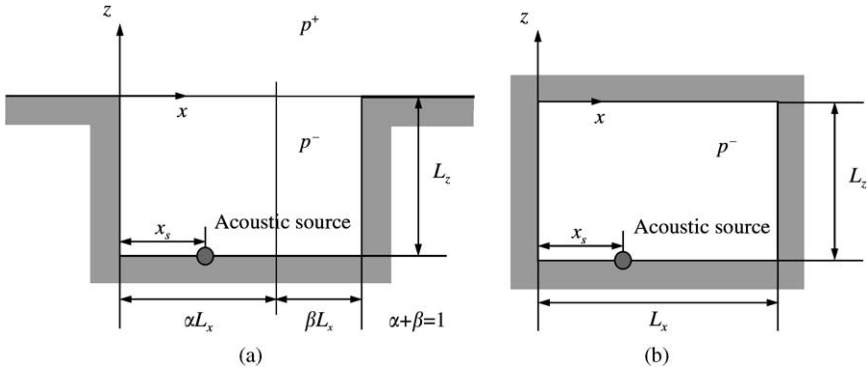

Figure 3. The two uncoupled systems that were used for the verification: (a) a partially opened cavity; (b) a closed cavity.

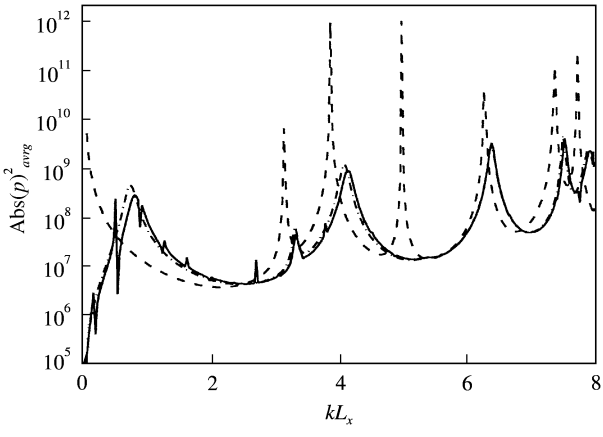

Figure 4. The spatially averaged sound pressure in the cavity: – – –, closed cavity; – · – · –, opened cavity; ——, coupling system.

effective to the system. The same phenomena occurs when $k_{zn}L_x$ has a very small value. This is because the size of the cavity relative to the z directional wavenumber is almost zero. Table 2 shows the limiting values of A_{mn} and B_{mn} for several cases.

5. NUMERICAL SIMULATIONS

In order to visualize the coupling system's behavior by using the equations derived, we performed several numerical simulations. For the verification of the equations, two uncoupled systems were also studied (Figure 3). The cavity size was 0·16 m × 0·13 m. The system was excited by a monopole source located at the bottom ($x = 0{\cdot}07$ m).

Figure 4 shows the pressure squared that is averaged over the cavity. We can see several sharp peaks for the closed cavity's case (dashed line). These peaks correspond to the cavity's natural frequencies. Table 3 compares several natural frequencies of the cavity system obtained by an analytic method with those obtained by the simulation. The discrepancy is due to the frequency resolution. Ten Hertz ($\Delta(kL_x) \approx 0{\cdot}03$) was used in the simulation. For

TABLE 3

Comparison of several natural frequencies of the system obtained by an analytic method and those obtained by the simulation ($\Delta f = 10$ Hz for numerical simulation)

Calculated natural frequency (Hz)	Natural frequency obtained by numerical simulation (Hz)	Mode (l, n)
1072	1070	(0, 0)
1319	1320	(1, 0)
1700	1700	(1, 1)
2144	2140	(2, 0)
2517	2520	(2, 1)
2638	2640	(0, 2)
2848	2850	(1, 2)

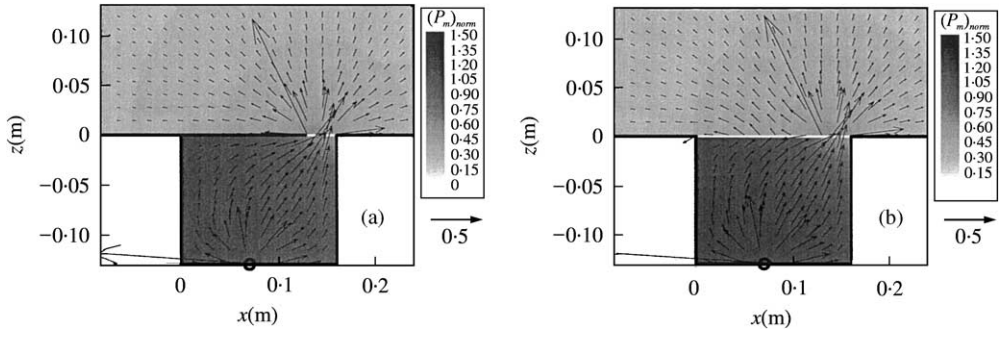

Figure 5. Contour and vector plots of acoustic fields at the first resonance frequency (frequency for the Helmholtz resonator mode), pressure and intensity are normalized by $\sqrt{\langle (p^-)^2 \rangle}$ and $\langle (p^-)^2 \rangle / 2\rho c^2$ respectively: (a) pressure and active intensity for the partially opened cavity at 250 Hz; (b) pressure and active intensity for the coupling system at 270 Hz.

the partially opened cavity (dash–dotted line, $\alpha = 0{\cdot}8$, the peaks have broader bandwidth than the ones of the closed cavity. This phenomenon is caused by the damping that results from a sound radiation to the exterior. The peak frequencies for the partially opened cavity are higher than those for the closed one. This is due to the change of boundary condition at the top surface. We can also observe the peak at $kL_x = 0{\cdot}733$ ($f = 250$ Hz). This corresponds to the Helmholtz resonator mode. The solid line (coupling system) has a trend similar to the result for the partially opened cavity except for several sharp peaks and troughs in the low-frequency range ($kL_x < 4$). In the frequency range lower than the frequency for the Helmholtz mode, the peak response occurs first and then the trough shows up as the frequency goes up. These orders are then reversed if the frequency is higher than the frequency of the Helmholtz mode. As shown in reference [15], these are very typical coupling phenomena that can be observed near the Helmholtz frequency.

Figure 5 shows the distributions of pressure and active intensity at the frequency for the Helmholtz resonator mode. The pressure is normalized by the square root of pressure squared averaged over the cavity ($\sqrt{\langle (p^-)^2 \rangle}$) and the active intensity is normalized by the value $\langle (p^-)^2 \rangle / 2\rho c^2$. The operator $\langle \cdot \rangle$ indicates the spatial average over the cavity. Because the walls and the baffle are rigid, active intensities normal to them is zero. For the partially opened cavity (Figure 5(a)), the power that emerges from the source goes out to the outer field through the hole. Figure 5(b) shows the results for the coupling system. The acoustic

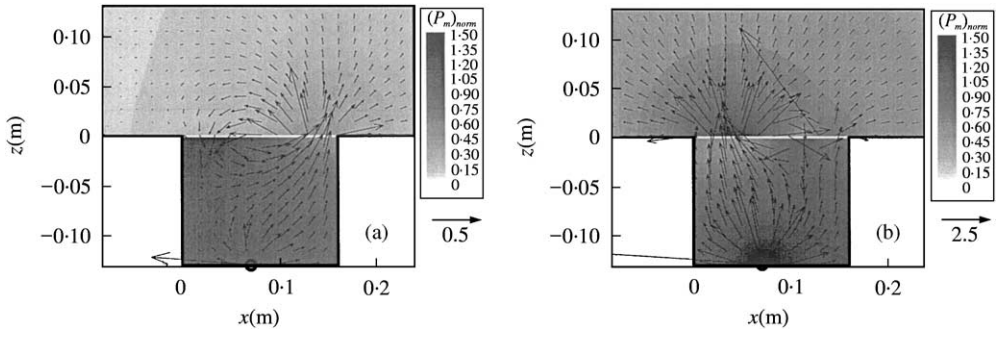

Figure 6. Contour and vector plots of acoustic fields for the coupling system at the second peak and trough frequencies, pressure and intensity are normalized by $\sqrt{\langle (p^-)^2 \rangle}$ and $\langle (p^-)^2 \rangle / 2\rho c^2$ respectively: (a) pressure and active intensity at the second peak (170 Hz); (b) pressure and active intensity at the second trough (180 Hz).

intensity plot indicates that the power goes out through the membrane as well as through the hole.

Figure 6 illustrates the distribution of pressure and active intensity at the second peak and trough frequencies (Figure 4). Same normalization was done as in Figure 4. At the peak frequency (Figure 6(a)), the entire energy from the cavity goes out to the exterior through the hole and some of it goes back to the cavity again. This energy circulation results in low radiation efficiency. However, at the trough frequency (Figure 6(b)) most energy goes out through the membrane. The pressures over the membrane have larger values than those over the hole. Active intensities at this frequency are larger than the ones at the peak frequency. These phenomena result due to the strong structural–acoustic coupling and confirms what was obtained by the experiments [15].

6. CONCLUSIONS

We derived the equation of motion that describes the sound pressure inside a finite cavity, the vibration amplitude of the membrane that partially covers the cavity, and the sound pressure of semi-infinite acoustic space. This physical configuration is believed to well represent a coupled acoustic problem. The coupled problem is indeed general because it enables us to study as to how the structure is coupled with finite cavity and exterior field, and how the hole is doing with them. Mathematically, it means that we have two boundary conditions on the surface of the interaction. The structure requires velocity continuity on and beneath it and the hole requires pressure and velocity continuity. This shows us that the number of unknowns are smaller than the number of equations. We solved this problem in the modal domain by additionally imposing the condition that requires sharing the internal cavity's modes by two coupling elements: structure and hole. The sharing law simply requires the same as possible modes number of the cavity as those of the coupling elements. The solution also provides the coupling coefficients. We believe those coefficients well represent the degree of coupling between four elements that we have handled: finite cavity, membrane, hole, and exterior field.

Numerical results reveal that the coupling slightly shifts Helmholtz frequency and makes a series of peak and trough sound pressure. We found that the peaks and troughs are symmetrically arranged with respect to Helmholtz frequency. The strong coupling is obtained at the trough frequencies where most of the energy goes out through the

membrane and high radiation efficiency is obtained. All the coupling effects described here are similar to the experimental results [15].

ACKNOWLEDGMENTS

This paper is partially supported by the Korea Science and Engineering Foundation (KOSEF, Project Number 98-0200-06-01-3), the Korea Institute of Science and Technology Evaluation and Planning (KISTEP, "National Research Laboratory" Project), and the Ministry of Education ("Brain Korea 21" Project).

REFERENCES

1. A. D. PIERCE 1994 *Acoustics: an Introduction to its Physical Principles and Applications*, 284–291. New York: Acoustical Society of America.
2. E. H. DOWELL and H. M. VOSS 1963 *American Institute of Aeronautics and Astronautics* **1**, 476–477. The effect of a cavity on panel vibration.
3. R. H. LYON 1963 *Journal of the Acoustical Society of America* **35**, 1791–1797. Noise reduction of rectangular enclosures with one flexible wall.
4. A. J. PRETLOVE 1965 *Journal of Sound and Vibration* **2**, 197–209. Free vibrations of rectangular panel backed by a closed rectangular cavity.
5. A. J. PRETLOVE 1966 *Journal of Sound and Vibration* **3**, 252–261. Forced vibrations of a rectangular panel backed by a closed rectangular cavity.
6. S. DE ROSA, F. FRANCO, F. MARULO, F. CONICELLA and G. ESPOSITO 1999 *Journal of Aircraft* **36**, 866–875. Full validation of the structural–acoustic response of a simple enclosure.
7. I. M. FIRTH 1977 *Journal of the Acoustical Society of America* **61**, 588–593. Physics of the guitar at the Helmholtz and first top-plate resonances.
8. G. CALDERSMITH 1978 *Journal of the Acoustical Society of America* **63**, 1566–1575. Guitar as a reflex enclosure.
9. O. CHRISTENSEN 1980 *Journal of the Acoustical Society of America* **68**, 758–766. Simple model for low-frequency guitar function.
10. G. VANDEGRIFT 1997 *Journal of the Acoustical Society of America* **102**, 622–627. The spatial inhomogeneity of pressure inside a violin at main air resonance.
11. G. BISSINGER 1998 *Journal of the Acoustical Society of America* **104**, 3608–3615. A0 and A1 coupling arching, rib height, and f-hole geometry dependence in the 2 degree-of-freedom network model of violin cavity modes.
12. A. F. SEYBERT, C. Y. R. CHENG and T. W. WU 1990 *Journal of the Acoustical Society of America* **88**, 1612–1618. The solution of coupled interior/exterior acoustic problems using the boundary element method.
13. R. W. GUY 1979 *Acustica* **43**, 295–304. The steady state transmission of sound at normal and oblique incidence through a thin panel backed by a rectangular room—a multi-modal analysis.
14. P. M. MORSE 1966 *Journal of the Acoustical Society of America* **40**, 354–366. Transmission of sound through a circular membrane in a plane wall.
15. S.-M. KIM and Y.-H. KIM 2001 *Journal of Acoustical Society of America* **109**, 65–74. Structural–acoustic coupling in a partially opened plate-cavity system: experimental observation by using nearfield acoustic holography.
16. O. CHRISTENSEN and B. B. VISTISEN 1980 *Journal of the Acoustical Society of America* **68**, 758–766. Simple model for low-frequency guitar function.
17. N. H. FLETCHER and T. D. ROSSING 1991 *The Physics of Musical Instruments*, 216–218. New York: Springer-Verlag.
18. A. D. PIERCE 1994 *Acoustics: an Introduction to its Physical Principles and Applications*, 180–183. New York: Acoustical Society of America.